J Braz. Soc. Mech. Sci. Eng. (2016) 38:385–394
DOI 10.1007/s40430-015-0341-5

TECHNICAL PAPER

# Displacement thickness evaluation for semi-empirical airfoil trailing-edge noise prediction model

**Joseph Y. Saab Jr.[1] · Marcos de Mattos Pimenta[1]**

Received: 19 November 2014 / Accepted: 13 March 2015 / Published online: 28 March 2015


**Abstract** This study proposes a criterion for evaluating the turbulent boundary layer displacement thickness when predicting airfoil trailing-edge noise with semi-empirical methods. The boundary layer integral parameter is usually employed as the typical turbulence length-scale in the classic NASA-BPM semi-empirical airfoil self-noise prediction model and its variations. Although the semi-empirical noise prediction methods have been, in theory, superseded by more complex and demanding simplified-theoretical methods, they arguably remain the most suitable methods for noise investigation during the preliminary design phase of airfoils and wind turbine blades. The purpose of the criterion discussed is to limit the adverse impact of the uncertainty associated with the scaling parameter into the overall intrinsic quality of the semi-empirical noise prediction method. The criterion may be then employed, along with computational efficiency, to sort out methods for the task of feeding the popular BPM noise prediction model and its variations. As an illustration of the application of the proposed criterion, the performance of CFD-RANS and XFoil codes are examined and compared with experimental data from turbulent, incompressible flow available from the literature in the range $5.0 \times 10^5 < \mathrm{Re_C} < 1.5 \times 10^6$.

Technical Editor: Fernando Alves Rochinha.

✉ Joseph Y. Saab Jr.
joseph.saab@usp.br

Marcos de Mattos Pimenta
marcos.pimenta@poli.usp.br

[1] Department of Mechanical Engineering, Polytechnic School, Sao Paulo State University (USP), Av. Prof. Luciano Gualberto, 530, Cidade Universitária, SP 05508-010, Brazil

**Keywords** Wind turbine noise · Airfoil trailing-edge noise · Displacement-thickness assessment

## List of symbols

### Latin letters

| | |
|---|---|
| $A$ | Empirical spectral shape based on the Strouhal number (dB) |
| $C$ | Airfoil chord (m) |
| $\bar{D}_\mathrm{h}$ | Directivity function, high-frequency noise () |
| $f$ | Frequency (Hz) |
| $K_1$ | SPL level experimental correction factor (dB) |
| $L$ | Span of the airfoil (m) |
| $M$ | Mach number () |
| OASPL | Overall sound pressure level (dB) |
| $\mathrm{Re_C}$ | Reynolds number, based on airfoil chord () |
| $r_\mathrm{e}$ | Effective observer distance (m) |
| $\mathrm{SPL_{1/3}}$ | Sound pressure level for a 1/3 octave band (dB) |
| $\mathrm{SPL_{p,\ 1/3}}$ | Sound pressure level for a 1/3 octave band, at pressure side (dB) |
| St | Strouhal number, $f\delta^*/U$ () |
| $\mathrm{St_p}$, $\mathrm{St_1}$ | Strouhal number, peak frequency () |
| TU | Turbulence intensity (% of U) |
| $U$ | Local mean velocity (m/s) |
| $U_\infty$ | Uniform flow velocity (m/s) |
| $Y^+$ | Wall coordinate, dimensionless distance to wall () |

### Greek letters

| | |
|---|---|
| $\alpha$ | Angle of attack (°) |
| $\delta^*$ | Boundary layer displacement thickness (m) |
| $\delta_p^*$ | Boundary layer displacement thickness, pressure side (m) |

| | |
|---|---|
| $k$ - $\omega$ | Turbulence model based on the turbulent kinetic energy and energy dissipation rate transport equations for mathematical closure |
| $\gamma$ - $Re_\theta$ | Transition model based on the intermittency factor and momentum thickness Reynolds number |

**Abbreviations**

| | |
|---|---|
| AOA | Angle of attack |
| BEM | Blade-element momentum theory |
| BL | Boundary layer |
| BPM | Brooks, Pope, Marcolini, NASA semi-empirical noise prediction model |
| CAA | Computational aero-acoustic (noise prediction models) |
| CFD | Computational fluid mechanics |
| HAWT | Horizontal axis wind turbine |
| IAG | Institut für Aerodynamik und Gasdynamik, Stuttgart |
| LE | Leading-edge |
| NREL | National Renewable Energy Laboratory, USA |
| POLI-USP | Polytechnic School of the University of Sao Paulo |
| RANS | Reynolds-averaged Navier–Stokes equations |
| R&D | Research and development |
| SE | Semi-empirical (noise prediction models) |
| SST | Shear stress transport |
| ST | Simplified-theoretical (noise prediction models) |
| TBL | Turbulent boundary layer |
| TBL-FP | Turbulent boundary layer over a flat plate model |
| TE | Trailing-edge |
| TU-Berlin | Technische Universität Berlin |
| WT | Wind turbine |
| WTN | Wind turbine noise |

## 1 Introduction

The noise emission from the trailing-edge (TE) of a wing is a classic problem in the fields of fixed and rotary-wing aircraft and has also become an additional design driver for wind turbines [36, 38].

The onshore wind energy conversion industry is developing swiftly in Brazil and most wind farms are being sited on the regions along the east coast, home for 85 % of the country population. Motivated by this fact, Poli-USP initiated an applied research on the wind turbine noise (WTN) subject to support R&D efforts for quieter wind turbine (WT) airfoils and blades.

An insight into the particular WT industry view of the noise problem was obtained through a field research carried out by the authors during an international wind power conference (AWEA 2012) and may be summarized by the closing comment of one large WT manufacturer expressed in his survey return form:

"It would be desirable to have routines for estimating aero noise in the early phases that could be later optimized in more advanced design phases. The better we can predict WTN, the easier we can assure our customers of the quality of our product. The industry lacks better predictive methods and also better ideas to lessen WTN".

Initially restricting the scope to self-noise and to the TE noise source only, which is considered the single most relevant source of airfoil self-noise for large size WT [37], the development of a noise prediction tool suitable for supporting the early conceptual design phase of airfoils and blades became the purpose of the application work initiated and two important goals were established for the tool to comply with expectations from the industry as expressed in the survey return forms: (i) the noise simulation tool would have to be practical enough for easy and highly iterative use during the early design phases of airfoil and blade designs, and (ii) the noise emission aspect should not be uncoupled from the rotor aerodynamic performance considerations.

This paper is concerned with some aspects of "phase one" of the method set-up, which consisted of the selection of the airfoil TE noise model plus a compatible flow field calculation tool to provide the characteristic wall-normal turbulence length scale required by the model. "Phase two" will be concerned with the blade/rotor TE noise prediction expansion and coupling to a performance analysis tool suitable for WT preliminary design and will be covered in a future text. The result of both phases will be incorporated into the QBlade open source WT performance software [33, 39], under collaborative effort with TU-Berlin. This is expected to grant easy Industry access to the tool and the new module shall preserve the proven, user-friendly interface of QBlade.

## 2 Trailing edge noise models

Some detailed studies are found in the literature concerning WT airfoil designing for reduced TE noise [3, 22, 23, 45]; however, some do not confirm the noise reduction expected from the airfoil geometry manipulations while others do not meet the high degree-of-freedom necessary for high iteration during the early design process.

Also, some blade and rotor (3-D) noise assessment tools have been designed with the clear intent to make them available to the Industry, especially by NREL [36], DTU [46] and also by Vargas [43]. All these are based on the BPM [10], 2-D semi-empirical (SE) noise prediction model and employ the "quasi 3-D" [20] approach that allows

extrapolation of the noise for the rotor by logarithmically summing up the sources in a number of blade stations and at different blade positions along the azimuthal plane, for each rotor speed. The main limitation of these tools, however, seems to be the use of the original BPM correlations for the displacement thickness developed for the NACA0012 and used as wall-normal turbulence length scales. NREL later coupled the model to the XFoil [13] to generalize the airfoil geometry [34] and also to its aeroacoustic code (FAST), however, for handling 2-D geometry only.

The simplified-theoretical (ST) models, most of which are based on the modified TNO-Blake TE noise model [26], have the potential to describe the noise that derives from the flow-edge interaction with much more physical detail than the SE models [35]. However, knowledge of the detailed turbulent flow field information is required for ST modeling, and the researchers often resort to two-equation turbulence models within CFD-RANS for that purpose plus modeling of the anisotropic turbulence properties and scaling functions. Examples of NREL and IAG researches in this area are [25–28, 31, 32, 35]. At the latest status report [24] the ST model seems less dependent upon empirical constants but the result is still very sensitive to the accuracy of the wall-normal turbulence length scale, as compared with the SE model. Although it currently represents the state-of-the-art on TE noise research in academia, the final advantage of the ST over the SE models, in terms of noise peak frequency and spectral shape prediction accuracy, seems not very well established and robust while the simpler SE models are more efficient from the computational point of view for iterative development research by the industry.

There are also high-order numerical models, like CAA, which are of less interest here because they have been a traditional barrier for the limited budget wind power industry as compared to the aerospace industry [14] and also too time consuming for preliminary investigation.

During selection of the elements for the intended practical WT TE noise prediction tool, both ST and SE models were considered in detail and the BPM model was selected as a starting point for the method due to its computational efficiency and reasonable accuracy. However, the model was not integrally adopted. Calculations of the typical operating conditions for a 50 m-radius HAWT with the aid of the BEM method [40], allowed conclusion that the Reynolds number at the outer 1/3 span of the rotor blades is in the range $1.5 \times 10^6 \leq \mathrm{Re_C} \leq 3.8 \times 10^6$ and hence operates in the same turbulent regime and not far from the experimental Reynolds number of data from which it was derived. This suggested that the boundary-layer integral parameter correlations provided with the model, derived specifically for the NACA 0012 airfoil were possibly its most critical limitation, especially considering the high camber, high adverse pressure gradient found in airfoils currently employed in WT design [41, 42]. For considerations on the model limitation concerning Reynolds number range applicability see [12], for instance.

Thus, it was concluded, in line with other authors [18, 36], that a successful effort to broaden the model applicability should involve substitution of a TBL flow field solver that could handle generic airfoil geometry operating in any AOA below the stall regime, for the original TBL fixed-geometry correlations provided by the model.

### 2.1 The BPM TE airfoil self-noise prediction model

Among noise relations for modeling all self-noise sources, the BPM model report [10] formulates three semi empirical relations for predicting the TBL TE noise based on flow measurements involving seven NACA 0012 airfoil models. The data for noise scaling were gathered within the very low turbulence ($TU \approx 0.05$ % at the center line) potential core of a jet flow discharging inside an external, anechoic chamber [9], and the general expression shape was based on the edge-scatter theoretical formulation of Ffowcs Williams and Hall [16]. The three semi empirical relations display the same general dependence on flow parameters as illustrated by Eq. (1).

$$\begin{aligned}\mathrm{SPL}_{\mathrm{p},1/3} = 10\log\left(\delta_{\mathrm{p}}^{*}M^{5}L\bar{D}_{h}/r_{e}^{2}\right) \\ + A\left(\mathrm{St_p}/\mathrm{St_1}\right) + (K_1 - 3) + \Delta K_1\end{aligned} \tag{1}$$

It may be seen from Eq. (1) that the noise pressure level at each 1/3 octave band depends logarithmically upon the TBL displacement thickness, $\delta^*$, which, for incompressible flow, is directly affected by Reynolds number and angle of attack,[1] $\delta^* = \delta^*(\alpha, \mathrm{Re})$. The displacement thickness is employed as a record of the development history of the turbulence over the airfoil. The relations $\mathrm{St_1} = 0.02M^{0.6}$, $K_1 = K_1(\mathrm{Re_C})$ and $\Delta K_1 = \Delta K_1(\alpha, \mathrm{Re_C})$ , are three empirical expressions that determine the peak Strouhal number, the peak $\mathrm{SPL}_{1/3}$ level and a correction factor for the SPL level, respectively. $A$ is an empirical spectral shape based on $\mathrm{Re_C}$.

By observing the typical plots of noise spectra of the original report [10], the method $\mathrm{SPL}_{1/3}$ prediction accuracy may be deduced to be within ±1 dB, from corrected measurements, at regions far from the peak frequency (depending upon flow speed), and a systematic +3 dB for frequencies in the vicinity of the peak frequency, for the range of velocities considered and zero α angle. For the OASPL prediction, the method and its variations are considered consistent: according to [27, p. 47], "these [BPM-based] models are quite popular, and the

[1] δ* is also affected by the freestream turbulence level, which determines transition, but the concern here is with airfoil self-noise only.

predictions of such models are in good agreement with measurements with a few decibel difference". Also [36], reported that the correlations kept within 3 dB from measured levels for lightly tripped boundary cases.

## 3 Developing a criterion for $\delta^*$ evaluation methods

### 3.1 Sensitivity analysis

By analyzing individual terms of the basic TE noise model, Eq. (1), it might seem at first that the displacement thickness variation would affect the first and second terms of the basic TE noise model equation, as shown in Eq. (2):

$$\partial \mathrm{SPL_p}/\partial\delta^* = \partial/\partial\delta^* \left[ 10 \log \left( \delta_p^* M^5 L \bar{D}_h / r_e^2 \right) + A\left(\mathrm{St_p}/\mathrm{St_1}\right) \right] \tag{2}$$

However, the Strouhal number ratio $\mathrm{St_p}/\mathrm{St_1}$ is calculated at the same physical location and also becomes independent of $\delta^*$. The role of the second term on the right side of Eq. (2) is to identify the shift of the specific 1/3 octave band under analysis in respect to the peak frequency, and to apply the appropriate roll-off. Thus, for a reference geometry and flow, a fixed 1/3 octave frequency band and a fixed-position observer (microphone) in relation to the airfoil TE, the relation may be further reduced to

$$\mathrm{SPL_{p,1/3}} = 10 \log \delta_\mathrm{p}^* + C_1, \tag{3}$$

where constant $C_1$ includes all the case, band and observer position (distance and angles for directivity function) fixed parameters.

The log dependence of $\mathrm{SPL_{p,1/3}}$ on $\delta_\mathrm{p}^*$, Eq. (3), shows that the sound pressure level will change arithmetically as the displacement thickness value changes geometrically, ceteris paribus. This relative insensitivity might explain why no studies were found in the literature about the quality of the TBL length scale estimation for BPM-type models, while for the ST models on the other hand, many authors have stressed the importance of the quality of the TBL parameters used in the models [25, 26, 31, 35]. Some of the most frequent approaches for TBL parameter calculation found in a broad bibliographical review of ST and SE noise prediction models are listed below in the order of increasing geometric flexibility and decreasing computational efficiency.

- TBL–flat plate correlation [21, 30].
- Experimental correlations developed by BPM [19, 36, 43].
- XFoil [2, 34, 46].
- CFD-RANS [21, 24, 29].

### 3.2 Quality criterion proposition

Although environmental certification of a WT siting requires a noise measurement procedure based on specific standards (e.g., IEC 61400-11, 2012), using appropriate, calibrated equipment and comparison with levels allowed by local regulations, it is reasonable to expect that during the preliminary design phase of a WT blade, the engineer would be willing to trade-off some accuracy in WTN prediction for speed, since the industry is interested in how small modifications of a given blade geometry will influence noise generation [44] and a large number of combination cases for testing is easily achieved. As a starting point aimed at the initial iterative design process, it is proposed as a discriminating criterion for evaluating $\delta^*$ calculation methods that the resultant departure of the displacement thickness from a reference value should not lead to an OASPL deviation of more than $\pm 3$ dB, estimated at a fixed (distance and angle) reference point, when applied to a BPM-type, TE noise prediction method. As mentioned, this criterion is not based on measurement equipment resolution, but rather on the time–accuracy tradeoff and also on psychoacoustic considerations, since this amount of SPL variation is considered "just perceptible" by a human being [4, p. 85], and prompts only a "marginal" increase in estimated public reaction to noise [4, 5]. Figure 1 is a plot of Eq. (3) and displays $\Delta\mathrm{SPL_{1/3}}$ (or $\Delta$OASPL) with $\delta^*$ relative value fluctuation, for this type of TE noise prediction method. It translates the proposed noise criterion into practical limits for $\Delta\delta^*/\delta^*$.

It may be seen from Fig. 1 that an underprediction by up to 50 % or overprediction by up to 100 % of the $\delta^*$, in respect to a reference value, would return OASPL within the limits required to meet this criterion ($\pm 3$ dB). Notice that, because the function is logarithmic, the upper and lower limits for $\delta^*$ % variation are not symmetrical and each doubling of the displacement thickness will increase the SPL by 3 dB. This is a typical SPL behavior perceived in the far-field from a compact noise source [4], making the displacement thickness analogous to a compact noise source in this model, which justifies the proposal of limits for its calculation process.

The criterion may be adjusted to match specific needs, e.g., an airfoil designer working on the conservative side could choose to work only on the OASPL overprediction side, i.e., up to +3 dB, for safe-design reasons. In this case, the designer should employ a displacement thickness estimation tool capable of reliably delivering values between *exact* and 100 % $\Delta\delta^*/\delta^*$ overprediction only.

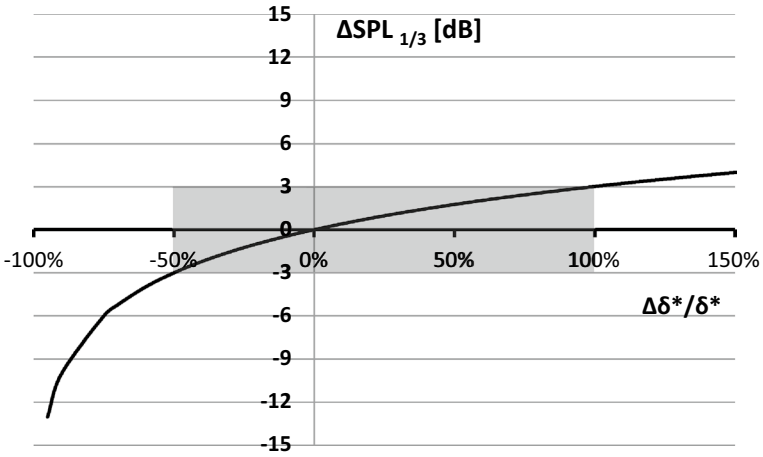


**Fig. 1** $SPL_{1/3}$ prediction variation with relative $\delta^*$ prediction variation, in a BPM-type noise model

## 4 Application of the proposed $\delta^*$ quality criterion

The aim of the intended modification to the original BPM TE noise prediction method, as briefly discussed, would be to extend its capability to any airfoil geometry by replacing a generic flow field solver for the original $\delta^*$ correlations. Any suitable flow field solver should be computationally efficient for intense iteration in the early design phase while meeting the proposed criteria of maximum SPL deviation for both fully turbulent and natural transition regimes. Although a geometric generalization is sought, the initial test of candidate methods is made against NACA 0012 data in zero AOA and chord-based Reynolds numbers for which experimental data are available from [8] and [10]. The two methods preselected for performance review, in light of geometric flexibility and popularity, were the XFoil (XFLR5 version) and incompressible CFD-RANS.

In the XFoil code, the steady Euler equations are employed in integral form to represent the inviscid flow and a compressible, integral method is used to represent the boundary layer and the wake. The viscous and inviscid flows are fully coupled through the displacement thickness [13]. The entire set of non-linear equations is solved simultaneously as a fully coupled system by the use of a global Newton–Raphson method. The software has been extensively validated for low and high α angles, e.g., [13, 17, 23] and has been quoted as the "standard tool" for the calculation of airfoil drag polar in the WT industry [33].

The airfoil chord was normalized for the different cases tested, and the resultant adjusted flow data for the reference experiments are displayed in Table 1.

### 4.1 XFoil modeling details

Because of the efficient computational approach and high frequency of referral found during the review of the noise prediction methods, the XFoil was tested first. The NACA 0012 airfoil surface was discretized into 300 panels, with larger panel concentration towards the TE and the LE. In the XFoil integral method, the skin friction and velocity profile formulas of Swafford [13] are employed in the turbulent regime and the $e^n$ criteria is employed for modeling transition flows, with $n = 9$ as default. The convergence was generally achieved in a few seconds for each operating point calculated.

**Table 1** Flow parameters for the reference cases tested in XFoil and CFD-RANS simulations, with a one-meter airfoil chord, zero α angle and TU of 0.05 % for all cases. Mach numbers are for dynamic TBL simulation purpose only and do not replace the original flow mach numbers in the BPM model

| Case[a] | U∞ (m/s) | Reynolds_*C* | Mach | References |
|---|---|---|---|---|
| B | 21.74 | 1.5E + 06 | 0.06 | [8, 10] |
| C | 16.93 | 1.2E + 06 | 0.05 | |
| D | 12.08 | 8.3E + 05 | 0.04 | |
| E | 9.67 | 6.6E + 05 | 0.03 | |
| F | 16.31 | 1.1E + 06 | 0.05 | |
| G | 10.87 | 7.5E + 05 | 0.03 | |
| H | 7.25 | 5.0E + 05 | 0.02 | |

[a] Letter "A" is reserved for a case of the main research text and was suppressed in this partial study because it refers to measurements accomplished at 96 % of the airfoil chord length [7] while all other cases listed had the measurements made at 100.13 % of the airfoil chord length

Both the original blunt TE NACA 0012 geometry [1] and a modified version with a sharp TE were initially tested. The displacement thickness results were linearly interpolated into the desired chord station from the closest neighboring discretization stations. The results for both TE configurations were similar, with the sharp TE values closer to experimental reference data.

### 4.2 CFD Modeling details

The flow around the NACA 0012 airfoil was modeled as a turbulent, incompressible, 2-D, steady flow, since the interest rests in integral TBL parameters and also a relatively swift method for deployment during the development phase of the airfoil.

The sharp TE NACA 0012 geometry was selected for the CFD simulation because it is also planned to be employed in future CAA aeroacoustic simulations, without the risk of including a tonal noise known as airfoil singing [6], which depends upon the TE bluntness parameter. This will preserve the same baseline geometry (but certainly not the discretization) for direct comparison of all the methods in the future.

Finite volume software ANSYS Fluent® was used throughout the simulations. The 2-D mesh architecture developed was an external D-grid with two internal stages of C-grids for progressive refinement. The far field defined was 12.5 chords long, aft and forward of the airfoil, with no less than 10 chords on the sides. The mesh was created with quadrilateral elements only and was refined until the first element was set at $Y^+ < 1$ from the airfoil surface and around 80 elements were embedded within the BL, resulting in 272,000 cell elements. The transition of elements was made smooth and the distortion of the elements controlled. The classical velocity inlet and pressure outlet boundary conditions were applied. After testing of some turbulence models, the SST, $k$ - $\omega$ model, plus $\gamma$ - $\mathrm{Re}_\theta$ transition equations, when applicable, were selected [40].

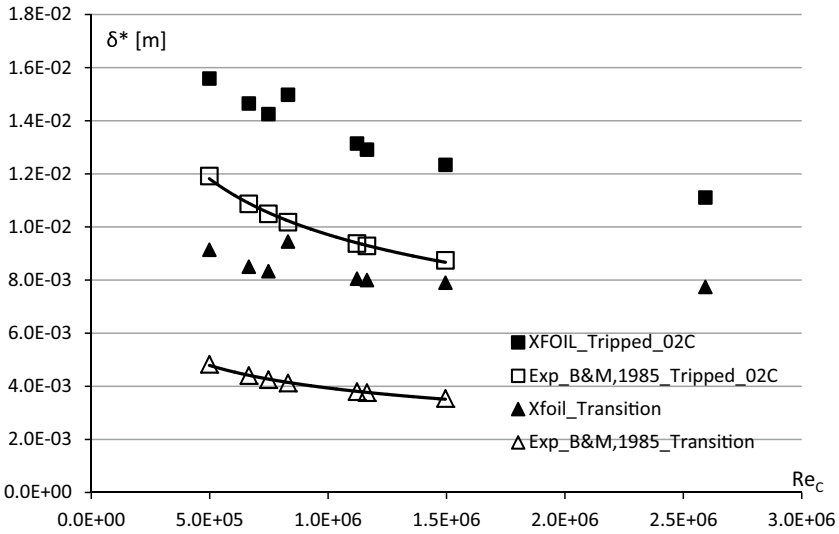


**Fig. 2** XFoil results for $\delta^*$, calculated for tripped and transition TBL, for the sharp TE NACA 0012 at station 1.0013C, in the range $5 \times 10^5 \leq \mathrm{Re_C} \leq 2.6 \times 10^6$

**Table 2** Relative error comparison for the XFoil results (tripped and transition TBL), for the sharp-TE NACA 0012 airfoil, in the range $5 \times 10^5 \leq \mathrm{Re_C} \leq 1.5 \times 10^6$

| XFoil validation and quality assessment–tripped and transition regimes | | | | | | | | | |
|---|---|---|---|---|---|---|---|---|---|
| Experimental | | | | XFoil | | Quality assessment | | | |
| Brooks and Marcolini [8] | | Heavily tripped | Natural transition | Sharp TE, tripped @ 0.2$C$ | Sharp TE, e^9 transition | Heavy tripping | e^9 transition | Heavy tripping | e^9 transition |
| Case | Reynolds_$C$ | δ* @ 1.3 mm downstream of TE | | δ* @ 1.0013$C$ | | Δδ*/δ* @ 1.0013$C$ | | ΔSPL = 10Log(1 + Δδ*/δ*) (dB) | |
| B | 1.5E+06 | 8.7E−03 | 3.5E−03 | 1.2E−02 | 7.9E−03 | 41 % | 123 % | 1.50 | 3.48 |
| C | 1.2E+06 | 9.3E−03 | 3.8E−03 | 1.3E−02 | 8.0E−03 | 39 % | 113 % | 1.43 | 3.27 |
| D | 8.3E+05 | 1.0E−02 | 4.1E−03 | 1.5E−02 | 9.5E−03 | 47 % | 129 % | 1.68 | 3.60 |
| E | 6.6E+05 | 1.1E−02 | 4.4E−03 | 1.5E−02 | 8.5E−03 | 35 % | 93 % | 1.30 | 2.86 |
| F | 1.1E+06 | 9.4E−03 | 3.8E−03 | 1.3E−02 | 8.1E−03 | 40 % | 112 % | 1.47 | 3.26 |
| G | 7.5E+05 | 1.0E−02 | 4.3E−03 | 1.4E−02 | 8.3E−03 | 36 % | 96 % | 1.33 | 2.92 |
| H | 5.0E+05 | 1.2E−02 | 4.8E−03 | 1.6E−02 | 9.1E−03 | 31 % | 89 % | 1.17 | 2.77 |

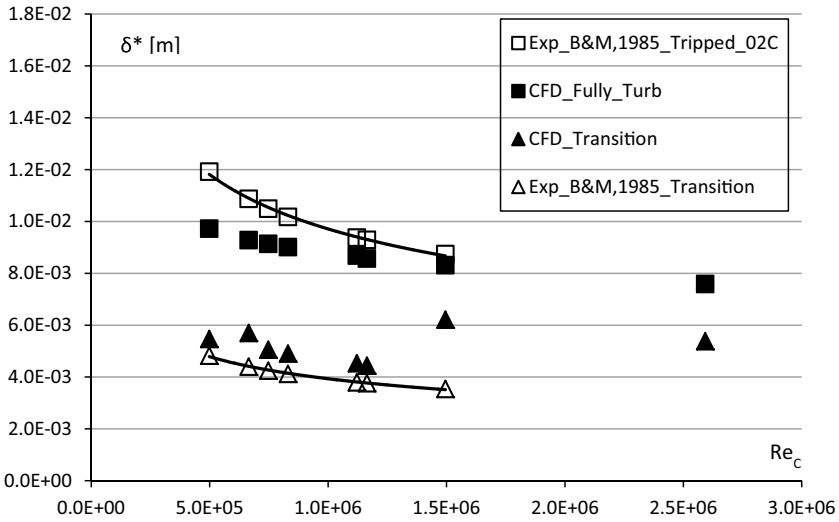


**Fig. 3** CFD simulations results for fully turbulent and transition cases, compared with experimental data of Brooks and Marcolini [8]

## 5 Results and discussion

### 5.1 XFoil results

Figure 2 displays the XFoil results for the tripped (at 0.2*C*) and transition TBL displacement thickness calculations, for Reynolds numbers in the range $5 \times 10^5 \leq \mathrm{Re_C} \leq 2.6 \times 10^6$, for the sharp TE NACA 0012 airfoil, measured downstream of the chord (1.0013*C*), plotted against experimental reference data.

The XFoil calculation results display physical behavior for both tripped and transition regimes, but there is a systematic overprediction of the displacement thickness when compared with the experimental reference data. This systematic shift behaves like an additional noise source and constitutes a typical situation for which the results should be first subjected to a quality evaluation, for example with the aid of the criterion laid out in this research, prior to being fed into a BPM-type TE noise prediction method.

From Table 2 it is possible to see that the XFoil results comply partially with the proposed criteria, when the calculation is done for station 1.0013*C*. The values for the heavy tripping situation are all acceptable in the Reynolds number range calculated, but those for transition TBL with relative deviations above 100 % would induce artificial noise sources in excess of 3 dB per 1/3 octave band in a BPM-type TE noise model.

### 5.2 CFD Results

The CFD simulation results for the range $5 \times 10^5 \leq \mathrm{Re_C} \leq 2.6 \times 10^6$ are shown in Fig. 3, along with the reference experimental results from [8]. The results also display physical behavior for both tripped and transition regimes and there is also a systematic shift when compared with experimental reference data. However, the shift is towards overprediction for points of the transition regime with low Reynolds numbers and towards underprediction in the fully turbulent regime cases, which are compared with experimental heavy tripping cases.

Once more this shifting prediction patterns require a criterion for acceptance and eventual use into a BPM-type TE noise prediction method.

Table 3 shows the quality assessment for all CFD cases, based on the criterion proposed in Sect. 3, for the calculations made for chord station 1.0013*C*. All displacement thickness results comply with the quality criteria proposed for further use in a BPM-type TE noise prediction model, i.e., all values are within $\Delta\delta^*/\delta^*$ proposed limits from +100 to −50 %. However, the run time necessary to solve all 16 plotted operating points and 4 error-study additional cases was close to 48 core-hours in a 3-GHz machine, or 2.4 core-hours per operating point.[2] The time necessary to develop and refine the mesh is an important additional concern for airfoil design iterative use and would be recurrent for every new airfoil geometry tested.

### 5.3 Discussion

Experimental data used in [10] are from [8] and have an associated uncertainty of less than ±5 % for the tripped cases and less than ±10 % for the natural transition cases. In order to formally compare the CFD results with experimental data, the quantifiable uncertainties associated with each of the flow types was considered. For this purpose, a study of the discretization error, based on the Richardson extrapolation [15], called the grid convergence method [11], was applied to the fully turbulent and transition solutions for one selected operating point, case F

[2] Average of 36 min per point in a four processor 3 GHz machine.

**Table 3** Relative error comparison for the CFD results (turbulent and transition TBL), for the sharp-TE NACA 0012 airfoil, in the range $5 \times 10^5 \leq \mathrm{Re_C} \leq 1.5 \times 10^6$

| CFD validation and quality assessment–fully turbulent and transition regimes | | | | | | | | | |
|---|---|---|---|---|---|---|---|---|---|
| Experimental | | | | CFD | | Quality assessment | | | |
| Brooks and Marcolini [8] | | Heavily tripped | Natural trans. | Sharp TE, fully turbulent | Sharp TE, re-theta transition | Turb. | Trans. | Turb. | Trans. |
| Case | Reynolds_$C$ | $\delta^*$ @ 1.3 mm downstream of TE | | $\delta^*$ @ 1.0013$C$ | | $\Delta\delta^*/\delta^*$ @ 1.0013$C$ | | $\Delta\mathrm{SPL} = 10\mathrm{Log}(1 + \Delta\delta^*/\delta^*)$ (Db) | |
| B | 1.5E+06 | 8.7E−03 | 3.5E−03 | 8.3E−03 | 6.2E−03 | −5 % | 76 % | −0.22 | 2.44 |
| C | 1.2E+06 | 9.3E−03 | 3.8E−03 | 8.6E−03 | 4.4E−03 | −8 % | 18 % | −0.35 | 0.72 |
| D | 8.3E+05 | 1.0E−02 | 4.1E−03 | 9.0E−03 | 4.9E−03 | −11 % | 19 % | −0.53 | 0.76 |
| E | 6.6E+05 | 1.1E−02 | 4.4E−03 | 9.3E−03 | 5.7E−03 | −15 % | 30 % | −0.69 | 1.12 |
| F | 1.1E+06 | 9.4E−03 | 3.8E−03 | 8.7E−03 | 4.5E−03 | −7 % | 19 % | −0.33 | 0.77 |
| G | 7.5E+05 | 1.0E−02 | 4.3E−03 | 9.1E−03 | 5.1E−03 | −13 % | 19 % | −0.60 | 0.76 |
| H | 5.0E+05 | 1.2E−02 | 4.8E−03 | 9.7E−03 | 5.5E−03 | −18 % | 13 % | −0.88 | 0.54 |

($\mathrm{Re_C} = 1.1 \times 10^6$). Two progressively refined meshes, with grid refinement factors of 1.51 and 1.33, were generated for this evaluation. After the CFD simulation was run again for operating point F on the new meshes, the displacement thickness at 1.0013$C$ was re-evaluated and the discretization relative error computed was estimated at −3.2 % for the turbulent $SSTk, \omega$ case and +0.8 % for the transition $SSTk, \omega$ case, based on the finest mesh. However, since the simulations for the other operational points were carried out with the coarser grid, a −4.8 % error for the turbulent and a −7.5 % error for the transition cases were evaluated, based on the Richardson extrapolation reference value.

Since the discretization relative error associated with the CFD data is smaller than the relative error for the experimental points, the analysis of the quality of the method would not be worsened by incorporating the uncertainty involved.

Although no formal error study was accomplished for the XFoil simulation, it is safe to assume that an integral method has a larger uncertainty associated with it than a second-order finite volume CFD method and it also became clear that the quality of the integral method was inconsistent for evaluating $\delta^*$ for subsequent use in a BPM-type TE noise prediction method. However, the computational efficiency and geometric flexibility advantages evidenced by the methodic simulations accomplished in XFoil were so overwhelming that it was deemed worthwhile to give the method a deeper look at.

As further simulations were accomplished, it was noticed that by making the calculations at stations further upstream, the systematic error displayed for the transition case, of +2.6 dB (±1 dB), could be partially offset. By moving the calculation from the wake (1.0013$C$) to the TE

**Table 4** Relative error comparison for the XFoil results (tripped and transition TBL), measured at station 0.98$C$, for the sharp-TE NACA 0012 airfoil, in the range $5 \times 10^5 \leq \mathrm{Re_C} \leq 1.5 \times 10^6$

| XFoil validation and quality assessment–tripped and transition conditions | | | | | | | | | |
|---|---|---|---|---|---|---|---|---|---|
| Experimental | | | | XFoil | | Quality assessment | | | |
| Brooks and Marcolini [8] | | Heavily tripped | Natural transition | Sharp TE, tripped @ 0.2$C$ | Sharp TE, e^9 transition | Heavy tripping | e^9 transition | Heavy tripping | e^9 transition |
| Case | Reynolds_$C$ | $\delta^*$ @ 1.3 mm downstream of TE | | $\delta^*$ @ 0.98$C$ | | $\Delta\delta^*/\delta^*$ @ 0.98$C$ | | $\Delta\mathrm{SPL} = 10\mathrm{Log}(1 + \Delta\delta^*/\delta^*)$ (dB) | |
| B | 1.5E+06 | 8.7E−03 | 3.5E−03 | 4.9E−03 | 2.7E−03 | −44 % | −23 % | −2.53 | −1.13 |
| C | 1.2E+06 | 9.3E−03 | 3.8E−03 | 5.1E−03 | 2.9E−03 | −45 % | −23 % | −2.57 | −1.12 |
| D | 8.3E+05 | 1.0E−02 | 4.1E−03 | 6.1E−03 | 3.5E−03 | −40 % | −14 % | −2.24 | −0.67 |
| E | 6.6E+05 | 1.1E−02 | 4.4E−03 | 5.9E−03 | 3.1E−03 | −45 % | −29 % | −2.62 | −1.47 |
| F | 1.1E+06 | 9.4E−03 | 3.8E−03 | 5.3E−03 | 2.9E−03 | −44 % | −23 % | −2.52 | −1.13 |
| G | 7.5E+05 | 1.0E−02 | 4.3E−03 | 5.8E−03 | 3.1E−03 | −45 % | −28 % | −2.60 | −1.43 |
| H | 5.0E+05 | 1.2E−02 | 4.8E−03 | 6.4E−03 | 3.4E−03 | −46 % | −29 % | −2.71 | −1.47 |

position (1$C$) and then gradually towards the LE position (0.98$C$, 0.96$C$), the XFoil predictions of $\delta^*$ values initially approached the experimental values and then departed from them again. At station 0.98$C$, less than 3 % of the chord upstream of the experimental measuring point, the calculated values were closer to the experimental reference data and acceptable by the proposed criteria for all cases and both type of flows, as shown in Table 4. This is a procedure analogue to correcting the SPL obtained from data at the original 1.0013$C$ station, by approximately −4dB to verify the proposed quality criterion.

This correction, however, is not generalized at this point for other airfoil geometries or AOA.

## 6 Conclusions

The basic BPM TE noise model equations were selected to try to compose another practical airfoil noise prediction tool that will be coupled with an aerodynamic performance analysis tool. However, the original $\delta^*$ correlations were discarded while pursuing higher geometry and flow independence. This resulted in the need to couple the model to a generic flow solver, compatible with the original model accuracy and also with some additional requirements imposed by the intended end-user, the WT industry.

At first, the typical BPM TE noise equation behavior was found to be quite insensitive to displacement thickness evaluation techniques, since the spectral peak and shape are determined by the model empirical functions. However, by proposing a ±3 dB OASPL as allowable prediction variation as a direct consequence of displacement thickness evaluation error, the criterion imposes restrictions with discriminating potential. The techniques best suited for the displacement thickness estimation task must be capable of producing $\delta^*$ values in the range from −50 to +100 % of the experimental reference values. The criterion may be easily adjusted to match specific needs.

In order to illustrate the application of the concept, detailed displacement thickness calculations were accomplished with the XFoil and CFD-RANS to evaluate fitness of the tools for the task. For the ranges of $Re_C$ tested, the displacement thickness estimated by CFD-RANS could be input into BPM-type SE airfoil TE noise with no significant impact on its original quality of prediction, for zero α angle, whether the simulated airfoil flow is fully turbulent or of the natural transition type. However, the computational efficiency demonstrated was not enough for highly iterative early design and also new meshes must be tailored for each new airfoil geometry variation conceived.

When uniform criteria were initially adopted and the interpolation of the calculated data was consistently made at station 1.0013$C$ for both the XFoil and CFD-RANS tools, the XFoil method did not show consistency for predicting results by the defined criterion: although the calculations were acceptable for the heavy tripped case, they were out of proposed limits for the transition cases. However, the XFoil is known to be very efficient for flow field calculations and if the 0.98$C$ station was chosen for interpolation, the excessive systematic prediction shift observed in downstream stations would collapse into the acceptable region for the cases and flow types tested.

With the procedure of reading TBL data upstream of the original station, equivalent to applying a suitable SPL correction, the XFoil deviation in predicting TE noise for each 1/3 octave band through a BPM-type model would be of the same order of magnitude of the CFD-RANS predictions but with a solution time three orders of magnitude smaller (2160 s for CFD against <5 s for XFoil, per point).

The error-limiting concept proposed is suitable for sorting between flow field tools, in the specific flow conditions described, and it is also capable of suggesting techniques for compensating systematic model shifts, thus allowing deployment of tools of large computational efficiency but that would seem otherwise unfit to the task, based on the proposed criterion.

This is an ongoing research that will be further expanded by verifying if the proposed criterion will hold for angles below and above the “switching angle”, and also through validation of the airfoil TE noise spectra predicted for airfoils other than the NACA 0012, at various AOA, against experimental data.

## References

1. Abbott I, Von-Doenhoff A (1959) Theory of wing sections, 2nd edn. Dover, New York
2. Bareiss R, Guidati G, Wagner S (1994) An approach towards refined noise prediction of wind turbines. Thessaloniki. In: Proceedings of the European wind energy association conference and exhibition, pp. 785–790
3. Bertanoglio F, Madsen HA, Bak C (2009) Experimental validation of the TNO trailing edge noise model and application to airfoil optimization, Roskilde, s.n
4. Bies DA, Hansen CH (2009) Engineering noise control, 4th edn. Spon Press, Abingdon
5. Bistafa SR (2011) Acústica Aplicada ao Controle de Ruído. Segunda ed. São Paulo: Edgar Blücher
6. Blake WK (1986) Mechanics of flow-induced sound and vibration. vol I ed. Academic Press, Orlando
7. Brooks T, Hodgson TH (1981) Trailing edge noise prediction from measured surface pressures. J Sound Vib 78(1):69–117
8. Brooks T, Marcolini M (1985) Scaling of airfoil self-noise using measured flow parameters. AIAA J 23(2):207–213
9. Brooks T, Marcolini M (1986) Airfoil trailing-edge flow measurements. AIAA J 24(8):1245–1251
10. Brooks T, Pope S, Marcolini M (1989) Airfoil self-noise and prediction, Langley: NASA Reference Publication, p. 1218

11. Celik I et al (2008) Procedure for estimation of uncertainty due to discretization in CFD applications. J Fluids Eng 130:1–4
12. Doolan C, Moreau D (2013) Review of NACA 0012 turbulence trailing edge noise data at zeero angle of attack. Denver Co, INCE Europe, pp 1–10
13. Drela M, Giles MB (1987) Viscous-inviscid analysis of transonic and low reynolds number airfoil. AIAA J 25(10):1347–1355
14. Eisele O, Pechlivanoglou G, Nayeri CN, Paschereit CO (2013) Experimental & numerical investigation of inflow turbulence on the performance of wind turbine airfoils. Proceeding of the ASME Turbo Expo 2013: Turbine Technical Conference and Exposition, GT2013, 3–7 June 2013, San Antonio, Texas, USA, pp 1–10
15. Ferziger J, Peric M (2002) Computational methods for fluid dynamics, 3rd edn. Springer-Verlag, Berlin
16. Ffowks Williams J, Hall L (1970) Aerodynamic sound generation by turbulent flow in the vicinity of a scattering half-plane. J Fluid Mech 40(4):657–670
17. Fuglsang P, Antoniou I, Sorensen N, Madsen A (1998) Validation of a wind tunnel testing facilitiy for blade surface pressure measurements. RISO, Denmark
18. Fuglsang P, Bak C (2004) Development of the Risø wind turbine airfoils. RISO, Roskilde
19. Fuglsang P, Madsen H (1996) Implementation and verification of an aeroacoustic noise prediction model for wind turbines. RISO, Roskilde R_867
20. Glegg S (1987) Significance of unsteady thickness noise sources. AIAA J 25(6):839–844
21. Glegg S, Morin B, Atassi ORR (2010) Using Reynolds-Averaged Navier-Stokes calculations to predict trailing edge noise. AIAA J 48(7):1290–1301
22. Göçmen T, Özerdem B (2012) Airfoil optimization for noise emission problem and aerodynamic performance criterion on small scale wind turbine. J Energy 04:36
23. Guidati G, Wagner S (2000) Design of reduced noise airfoils for wind turbines, Barcelona, s.n
24. Kamruzzaman M et al. (2014) Rnoise: A RANS based airfoil trailing-edge noise prediction model. Atlanta, GA, 20th AIAA/CEAS Aeroacoustics Conference
25. Kamruzzaman M, Lutz T, Herrig A, Krämer E (2012) Semi-Empirical modeling of turbulent anisotropy for airfoil self-noise predictions. AIAA J 50(1):46–60
26. Kamruzzaman M, Lutz T, Nübler K, Krämer E (2011) Implementation and verification of an aeroacoustic wind turbine blade analysis tool. INCE Europe, Rome, pp 1–16
27. Kamruzzaman M et al (2012) Validations and improvements of airfoil trailing-edge noise prediction models using detailed experimental data. Wind Energy 15:45–61
28. Kamruzzaman M et al (2010) Wind turbine aerodynamics and aeroacoustics at University of Stuttgart–an overview of research and development. IAG, Stuttgart
29. Lockhard DP (1999) An overview of computational aeroacoustic modeling at NASA Langley. NASA, Hampton, pp 1–14
30. Lowson M (1993) Assessment and prediction of wind turbine noise, Bristol: ETSU W/13/00284/REP USDOE
31. Lutz T, Herrig A, Kamruzzaman M, Krämer E (2007) Design and wind-tunnel verification of low-noise airfoils for wind turbines. AIAA J 45(4):779–785
32. Lutz T et al (2004) Numerical optimization of silent airfoil sections. Wilhemshaven, Deutsches Windenergie
33. Marten D (2010) Extension of an aerodynamic simulator for wind turbine blade design and performance analysis. TU Berlin, Berlin
34. Moriarty P (2005) NAFNoise user's guide. NREL, Golden
35. Moriarty P, Guidati G, Migliore P (2005) Prediction of turbulent inflow and trailing-edge noise for wind turbines. AIAA, Monterrey, pp 1–16
36. Moriarty P, Migliore P (2003) Semi-empirical aeroacoustic noise prediction code for wind turbines. NREL, Golden
37. Oerlemans S (2011) Wind turbine noise: primary noise sources. Nationaal Lucht-en Ruimtevaartilaboratorium–NLR, Amsterdam
38. Oerlemans S, Fisher M, Maeder T, Kögler K (2009) Reduction of wind turbine noise using optimized airfoils and trailing-edge serrations. AIAA J 47(6):1470–1481
39. Pechlivanoglou G et al. (2009) QBlade, Berlin, s.n
40. Saab JY Jr, Pimenta M (2014) Airfoil self-noise–development of a trailing edge noise prediction tool suitable for the preliminary aeroacoustic design of quieter wind turbine blades. EPUSP, Sao Paulo
41. Somers D, Tangler J (2005a) The S822 and S823 airfoils, Golden, NREL/SR-500-36342
42. Somers D, Tangler J (2005b) The airfoils S830, S831 and S832, Golden:NREL/SR-500_36339
43. Vargas LFC (2008) Wind turbine noise prediction. Instituto Superior Técnico, Lisboa
44. Wagner S, Bareiß R, Guidati G (1996) Wind turbine noise, 1st edn. Springer, Berlin
45. Wolf A et al. (2011) Trailing edge noise reduction of wind turbine airfoils by active flow control. Rome, s.n., pp. 1–12
46. Zhu W (2004) Modelling of noise from wind turbines. DTU, Lyngby